JOURNAL OF OPTOELECTRONICS AND ADVANCED MATERIALS Vol. 13, No. 6, June 2011, p. 706 - 712

Structural phase transition and mechanical properties of SmAs under high pressure

SADHNA SINGH*, P.J. JOFFY, M. FAISAL SHAREEF
High Pressure Research Lab, Department of Physics, Barkatullah University, Hoshangabad Road , Bhopal- 462026, India

High pressure phase transition and mechanical properties of SmAs which crystallize in NaCl (B1) structure has been investigated using the three body interaction potential (TBIP) approach. These interactions arise due to the electron shell deformation of the overlapping ions in the crystals. The TBIP model consists of long range Coulombic, three body interaction and the short range overlap repulsive forces operative up to next nearest neighbor ions. During phase transition there is an intermediate tetragonal phase which can be viewed as distorted CsCl (B2) structure and finally it transforms to CsCl (B2) phase at phase transition pressure. The values of phase transition pressure, associated volume collapse, bulk modulus and its pressure derivative estimated by us are found to be well suited with experimental values. Thus TBPIM is in good agreement with their available measured data. In view of its overall success, it can be regarded as an adequate and appropriate model suitable for high pressure studies.

(Received July 27, 2010; accepted June 9, 2011)

Keywords: High Pressure, Phase transition, Three body interaction, Volume Collapse, Elastic Properties

1. Introduction

The high pressure structural behavior of binary AB compounds with NaCl type structure has been a popular topic in condensed matter research. Among these compounds rare earth monopnictides show diversity in their electronic, magnetic and structural properties. Their high pressure structural behaviour has attracted a great attention in the research field both theoretically and experimentally [1-4]. Rare Earth monopnictides are generally semiconductors and semimetals. Despite their simple rock salt structure, they demonstrate various types of magnetic ordering generally with low transition temperature .Their electronic structure and magnetic properties are sensitive to temperature, pressure and impurity effects. The rare earth 4f – 5d interactions and the hybridization between the rare earth and non – 4f and pnictogen p states are responsible for many fascinating phenomena that occur in rare earth monopnictides [5]. Most of the rare earth monopnictide compounds crystallize in cubic NaCl (B1) type structure at ambient pressure but undergo a phase transition to a CsCl (B2) structure under high pressure. These transitions result in the increase in coordination number from 6 to 8. These studies have correlated the unusual physical properties of these compounds to the f-electron hybridization with the conduction electrons and also due to the strong mixing of the f-states of the rare earth ion with the neighboring p-orbital of the anion (p-f mixing). The $B1 \rightarrow B_2$ transition is of considerable importance as a model for other structural phase transformations. It is one of the simplest first order transitions.

The structural properties of CeAs, NdAs, PrAs and SmAs, compounds have been investigated recently [6-8] in great detail. The salient features of SmAs were observed by Shirotani et al. [1] from their high-pressure X-ray diffraction experiments. This compound crystallizes in B1 structure .The high- pressure form of the SmAs is a tetragonal structure and can be viewed as a distorted CsCl-type structure. They reported phase transition in SmAs at 32.1 GPa. The aim of the present work is the investigation of phase transition pressure, volume collapse, second order elastic constants and their combinations, elastic modulii, and pressure derivatives of elastic modulii of SmAs.

In order to achieve this goal, we have formulated a three-body interaction potential (TBIP) [9,10], which consists of the long-range Coulomb and three-body interactions and Born-Mayer overlap repulsion operative up to next nearest neighbor ions. A brief account of the theoretical approach is presented in section 2. The results are discussed in section 3.

2. Potential model and method of computation

The three body interaction arises when, during lattice vibrations, electron shells of neighboring ions overlap. This overlapping leads to the transfer of charge which when interacts with other charges, many body interaction (MBI) takes place, the dominant part of MBI is three body interactions. Application of pressure on crystals results in compression which leads to an increased charge transfer (or three body interaction effects) due to the deformation of the overlapping electron shells of the adjacent ions (or non rigidity of ions) in solids .So three body interactions become more important when we apply pressure on our compound. Thus Columbic energy gets modified because of the presence of three body interactions (TBI) which is dependent on the nearest neighbor as

$$f(r) = f_0\, exp\left(\frac{-r}{\rho}\right) \qquad (1)$$

These effects have been incorporated in the Gibbs free energy, given by

$$G = U + PV - TS \qquad (2)$$

Where U is the internal energy which at 0K corresponds to the cohesive energy (lattice energy), S is the vibrational entropy at absolute T, pressure P and volume V. The Gibbs free energies G_{B1} for the NaCl (B1) and G_{B2} for the CsCl (B2) phases become equal at the phase transition pressure P,

$$G_{B1}(r) = U_{B1}(r) + PV_{B1} \qquad (3)$$

$$G_{B2}(r') = U_{B2}(r') + PV_{B2} \qquad (4)$$

With V_{B1}(=2.00 r^3) and V_{B2}(=1.54 r'^3) as the unit cell volumes for B1 and B2 phases respectively. The first terms in the energies (3) and (4) are lattice energies for B1 and B2 structure and they are expressed as

$$U_{B1}(r) = -\alpha_m z^2 e^2 / r - (12\alpha_m z e^2 f(r))/r + 6b\beta_{ij}\exp[(r_i + r_j - r)/\rho] + 6b\beta_{ii}\exp[(2r_i - 1.414r)/\rho] + 6b\beta_{jj}\exp[(2r_j - 1.414r)/\rho] \qquad (5)$$

$$U_{B2}(r') = -\alpha'_m z^2 e^2 / r' - (16\alpha'_m z e^2 f(r'))/r + 8b'\beta_{ij}\exp[(r_i + r_j - r')/\rho] + 3b'\beta_{ii}\exp[(2r_i - 1.154r')/\rho] + 3b'\beta_{jj}\exp[(2r_j - 1.154r')/\rho] \qquad (6)$$

Here, the first term in the above equations (5) and (6) is a long range Coulomb energy and the second term is due to three –body interactions corresponding to the nearest neighbor separation $r(r'), \alpha_M(\alpha'_M)$ are the Madelung constants for B1(B2) phases. The remaining terms correspond to the overlap repulsion represented by Hafemeister and Flygare (HF) type potential and extended up to the next nearest neighbor ion, with b and ρ being the hardness and range parameters, β_{ij} the Pauling coefficient. The cation (anion) radii are given by $r_i(r_j)$, Ze is the ionic charge , $f(r), f(r')$ are the TBI parameters for B1(B2) phases .

There are three model parameters (b, ρ, f(r)) involved in the present TBP, namely hardness, range and three-body force parameter respectively. Their values have been determined by solving the equilibrium conditions,

$$\left[\frac{du}{dr}\right]_{r=r_0} = 0$$

and

$$\left[\frac{d^2u}{dr^2}\right] = 9kr_0B_T \qquad (7)$$

Here, B_T is isothermal bulk modulus and k=2 for B1 phase. Accordingly, the value of hardness parameter increases by the ratio $\frac{8}{6}$ for B1 phase [11] as

$$b' = \frac{8}{6}b \qquad (8)$$

Here, number 8 and 6 are the coordinate number for B2 and B1 structures respectively.

Let us consider the conditions for the pressure induced transformation. This is achieved at absolute zero of temperature because the energy description is not sufficiently sophisticated to take care of the vibrational contribution to entropy at other temperatures. At absolute zero, the Gibbs free energy (G) is the enthalpy (H) itself. For any two structures real (B1) and hypothetical (B2) at phase transition pressure (P), we have

$$G_{B1}(r) = G_{B2}(r') \qquad (9)$$

The Gibbs free energy of (B1) and (B2) phase is given in equations (3) and (4). The internal energy (cohesive energy at absolute zero) from the given phase is given by the equations (5) and (6).

As an isolated phase is stable only if its free energy is at minimum, we have adopted the method of minimization of free energies for both the phases. At the phase transition pressure, the difference of free energies (ΔG) approaches zero .The pressure at which ΔG→0 is called the phase transition pressure. The associated volume with this pressure shows a sudden collapse in volume showing that the phase transition is of first order.

The relative volumes, $\frac{V(P)}{V(0)}$ (Here, V(P) is the volume of the material at applied pressure P in NaCl/CsCl phase and V (0) is the volume at P=0 i.e. in NaCl phase) have been computed and plotted against the pressure in fig. 2 to get the phase diagrams and volume collapses, $\frac{\Delta V(P_t)}{V(0)}$(Here, $\Delta V(P_t)$ is the difference in volumes of two phases at P_t), associated with the phase transitions.

To understand the elastic properties of the SmAs we have calculated second order elastic constants (C_{11}, C_{12} and C_{44}) and their pressure derivatives, since these elastic constants are the functions of first and second order derivatives of short-range potential, so their calculation will provide knowledge about the effect of short-range forces on these materials following Shanker et al. [12] and the expression followed by Singh et al. [13].

The expressions for second order elastic constants are as follows

$$C_{11} = (e^2/4a^4).[-5.112Z\,(Z+12f(r)) + A_1 + (A_2+B_2)/2 + 9.3204Zaf(r)] \quad (10)$$

$$C_{12} = (e^2/4a^4).[0.226\,Z\,(Z+12f(r)) - B_1 + (A_2-5B_2)/4 + 9.3204Zaf(r)] \quad (11)$$

$$C_{44} = (e^2/4a^4).[2.556\,Z\,(Z+12f(r)) - B_1 + (A_2+3B_2)/4] \quad (12)$$

In equations (10)-(12), first term represents the long range coulomb interaction, second term represents the contribution due to TBIP and remaining contribute overlap repulsion expressed in terms of the short-range parameters (A_1, B_1) and (A_2, B_2) for the nearest neighboring (nn) and next nearest neighboring(nnn) ions.

The compressibility (β), which is mainly used in earth science to quantify the ability of a soil or rock to reduce in volume with applied pressure. It can be obtained as the reciprocal of bulk modulus of the cubic crystal and can be expressed as,

$$\beta = 1/B_T = 3/(C_{11} + 2C_{12}). \quad (13)$$

The combination of the second order elastic constants have also calculated using the relations,

$$C_s = (C_{11} - C_{12})/2 \quad (14)$$

and

$$C_L = (C_{11} + C_{12} + 2C_{44})/2 \quad (15)$$

Where C_S is the shear modulus of the crystal and C_L is the Tetragonal modulus of the crystal.

It is known that even the cubic crystal which is isotropic structure, also has elastic anisotropy as a result of a fourth rank tensor property of elasticity. The Zener anisotropy factor (A), Young's Modulus (Y), often referred to simply as the elastic modulus, and the Poisson's ratio (ν), which are the most interesting elastic properties for applications, are also calculated in terms of the computed data of second order elastic constants using the following relations [14].

$$A = 2\,C_{44}/(C_{11}-C_{12}) \quad (16)$$

$$Y = 9GB/(G+3B) \quad (17)$$

and

$$\nu = 1/2\,[(B-2/3G)/(B+1/3G)] \quad (18)$$

where $G = (G_V+G_R)/2$ is the isotropic shear modulus, G_V is Voigt's shear modulus corresponding to the upper bound of G values, and G_R is Reuss's shear modulus corresponding to the lower bound of G values, and can be written as

$$G_V = (C_{11}-C_{12}+3C_{44})/5 \quad (19)$$

and

$$5/G_R = 4/(C_{11}-C_{12})+3/C_{44}. \quad (20)$$

The pressure derivative of elastic modulii is calculated using the following equations [15, 16].

$$\frac{dB}{dP} = -(3\Omega)^{-1}[13.980Z(Z+12f(r)) + c_1 - 3A_1 + C_2 - 3A_2 - 167.76448Zaf'(r) + 41.9420Za^2 f''(r)] \quad (21)$$

$$\frac{ds}{dP} = -(2\Omega)^{-1}[23.682Z(Z+12f(r)) + C_1 + (C_2 + 6A_2 - 6B_2)/4 - 50.0752zaf'(r) + 13.9808za^2 f''(r)] \quad (22)$$

$$\frac{dC_{44}}{dP} = -(\Omega)^{-1}[-11.389Z(Z+12f(r)) + A_1 - 3B_1 + (C_2 + 2A_2 - 10B_2)/4 + 44.6528Zaf'(r) \quad (23)$$

Where

$$\Omega = -2.330Z(Z+12f(r)) + A_1 + A_2 + 21.9612Zaf'(r)$$

The values of A_i, B_i have been calculated from the knowledge of *b* and ρ.

3. Results and discussions

The input crystal data and calculated model parameters $[b, b', \rho, f(r)]$ of SmAs are given in table 1 and 2 respectively. Using model parameters and minimization technique, transition pressure (P_t) has been predicted. We have minimized Gibb's free energies for real (B1 before P_t and B2 after P_t) and hypothetical (B2 before P_t and B1 after P_t) phases for different pressures.

Table 1. Input crystal data of SmAs

Compound	Input Parameters			
	$r_i(A^0)$*	$r_j(A^0)$*	$r_o(A^0)$**	B_T(GPa)**
SmAs	0.89	1.2	2.9605	84.2

* Ref. [17] ** Ref. [1]

Table 2. Model parameters of SmAs

Compound	Model parameters			
	b(10^{-12}ergs)	b'(10^{-12}ergs)	$\rho(A^0)$	f(r)
SmAs	5.5544	7.4059	0.348	-0.0095

Now we have evaluated the corresponding Gibb's free energy difference $\Delta G(= G_{B1} - G_{B2})$.We have plotted ΔG against pressure (P) for SmAs in fig. 1. As the pressure is increased, ΔG decreases and approaches to zero at the phase transition pressure. From fig. 1 it is clear that the phase transition pressure for SmAs is 32.6 GPa. The experimental value 32.1 GPa [1] is also shown in figure and noted that our value is in good agreement with experimental data and is better than the previous workers, G. Pagare et al. [17].

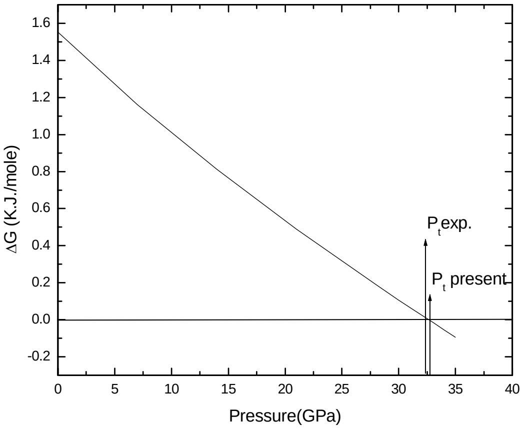

Fig. 1. Variation of Gibbs free energy difference ΔG (KJ/mol) with pressure for SmAs. Represented by solid lines.

The relative volumes, $\frac{V(P)}{V(0)}$ (Here, V(P) is the volume of the material at applied pressure P in NaCl/CsCl phase and V (0) is the volume at P=0 i.e. in NaCl phase) have been computed and plotted against the pressure in fig. 2 to get the phase diagrams and volume collapses. The values of these volume collapses along with their experimental results are listed in table 3 for SmAs. The magnitude of relative volume change at the transition pressure for SmAs is 8.53 % which is in good agreement with those from experimental approach which are given in table 3 and fig. 2. The experimental results are shown by solid squares (■) in fig. 2 and they are showing the same trend as our values.

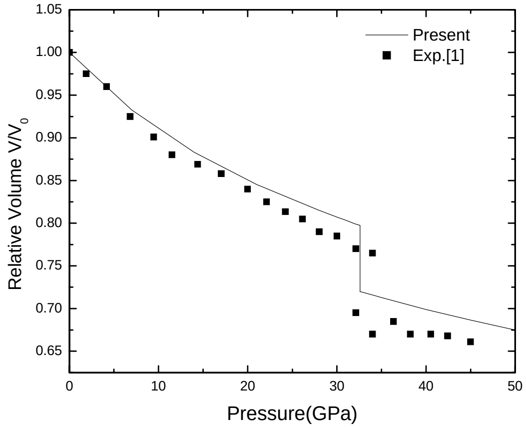

Fig. 2. Variation of volume change $V_p/V_0$with pressure for SmAs. Solid line represents the present value and solid squares (■) represent the experimental value [1].

Table 3. Calculated transition pressure and volume collapse SmAs

Compound	Transition	Transition pressure(GPa)			Volume collapse (%)		
		Present	Expt.**	Others*	Present	Expt.**	Others*
SmAs	B1→B2	32.6	32.1	33.3	8.53	10	11

* Ref. [17] ** Ref. [1]

The elastic constants of solids provide a link between the mechanical and dynamical behavior of crystals, and give important information concerning the nature of the forces operating in solids. In particular they provide information on the stability and stiffness of materials.We have calculated second order elastic constants (SOEC)- C_{11}, C_{12} & C_{44} and their combinations C_L & C_S. The quantities C_S & C_L are the shear and tetragonal modulii of a cubic crystal respectively. These are given in table 4. The elastic constant C_{11} represents elasticity in length. That is a longitudinal strain produces a change in C_{11}. The elastic constants C_{12} and C_{44} are related to the elasticity in shape, which is a shear constant. A transverse strain causes a change in shape without a change in volume. Therefore C_{12} and C_{44} are less sensitive to pressure as compared to C_{11}. It is necessary for lattice to satisfy Born criterion for mechanically stable state. For this purpose, the elastic energy density must be a positive definite quadratic function of strain. In order to fulfill the above criterion, the principal minor (eigen values) of the elastic constant matrix should all be positive. Vukcevich [18] also stated the high pressure stability criterion for ionic crystal, the stable phase of a crystal is one in which the shear elastic constant C_{44} is non-zero (for mechanical stability) and which has the lowest potential energy among the mechanically stable lattices. Thus, the stability of NaCl-type structure in terms of elastic constants should satisfy the following conditions:

$$B_T = (C_{11}+ 2C_{12})/3 > 0, \qquad C_{44} > 0, \qquad (24)$$

and

$$C_S = (C_{11}-C_{12})/2 > 0$$

From table 4 our estimated values of $C_{44} = 1.0670\times10^{12}$dyne/cm^2 and $C_S = 0.3708\times10^{12}$dyne/cm^2 for SmAs are positive and hence the above stability criterion is satisfied for ionic crystal.

Table 4. Second order elastic constants and their combinations (x10^{12}dyne/cm^2).

Compound	**C_{11}**	**C_{12}**	**C_{44}**	**Cs**	**C_L**
SmAs	1.3261	0.5846	1.0670	0.3708	2.0224

Besides this the values of Zener anisotropy factor, Young's modulus, Poisson's ratio and compressibility are calculated, and also noticed that the calculated compressibility is in good agreement with the experimental value. These are listed in the table 5. The pressure derivatives of second order elastic constants and their combinations are important for predicting the high pressure behavior. The pressure derivative of bulk modulus of SmAs is also given in table 6. It is clear from table 6 that our calculated value of pressure derivative of bulk modulus of SmAs is in good agreement with the experimental values.

Table 5. Moduli of Elasticity of SmAs

Compound	β (Gpa)$^{-1}$		A	Y (10^{12}dyne/cm^2)	ν
	Present	Experimental**			
SmAs	0.0120	0.0119	2.8780	0.0609	0.3060

** Ref. [1]

Table 6. Pressure derivaties of elastic modulii

Compound	$d B_T /dP$			dCs/dp	dC_{44}/dP
	Present	Expt.**	Others*		
SmAs	4.243	4.5±0.3	4.7	3.2665	-0.1584

The fig. 3 shows the variation of Sm-As distance with high pressure for the SmAs compound the distance between Sm-As ions is 2.96 A^0 at ambient pressure. At B1-B2 phase transition pressure of about 32.6 GPa the Sm-As distance suddenly increases and become 2.89 A^0 in B2 structure.

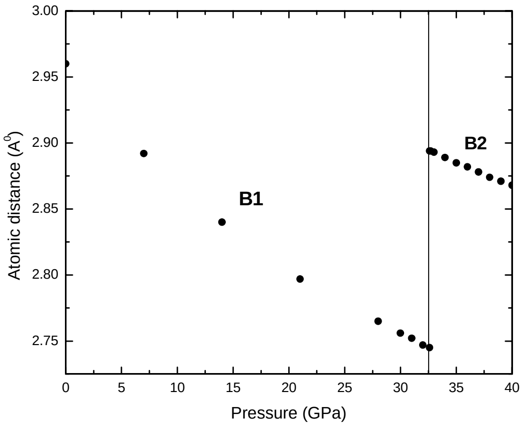

Fig. 3. Variation of Atomic distance with Pressure for SmAs at B1 and B2 phases. Represented by solid circles (●).

The fig. 4 shows the transition pressure against lattice constant in SmAs and in some other arsenides having B1 structure and showing B1-B2 transition under pressure. The present value of SmAs and the calculated value [8] of the NdAs have been compared with experimental values [1]. The transition pressure of the SmAs and NdAs increase with decreasing lattice constant and they have good agreement with experimental data.

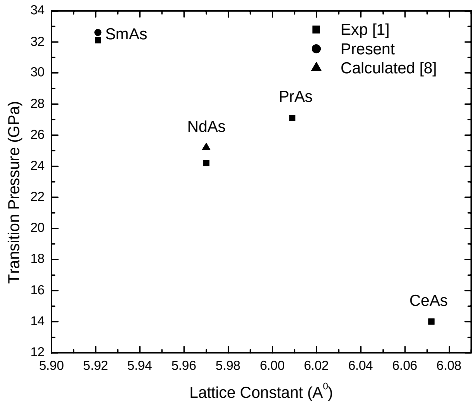

Fig. 4. Variation of transition pressure against lattice constant. solid circles (●), solid triangles (▲) and solid squares (■) represents present value,calculated value [7] and experimental values [1] respectively.

On the basis of above work we conclude that the TBP Model is adequately suitable for the prediction of B1 → B2 phase transition pressure, associated volume collapse, second order elastic constants and it's combinations, compressibility, anisotropy factor, Young's modulus, Poisson's ratio and pressure derivatives of bulk modulus, shear modulus, tetragonal modulus in SmAs. This approach may be applied to other lanthanide monopnictides for the study of phase transition phenomenon.

Acknowledgements

The authors are thankful to BRNS, Mumbai for financial support of this project.

References

[1] I.Shirtotani, K.Yamanashi, J.Hayashi, Y.Tanaka, N.Ishimatsu, O.Shimomura and T.Kikegawa. J.Phys:Condens.Matter **13**, 1939 (2001).

[2] I. Shirotani, J. Hayashi, K. Yamanashi, N. Ishimatsu, O. Shimomura, T. Kikegawa. Phys. Rev. B **64**, 132101 (2001).

[3] S.J. Allen, D Brehmer and CJ Palmstrom, 1993, Rare Earth Doped Semiconductors Vol 301ed. G.S. Pomrenka, P.B Klein and D W Langer (Pittsburg, PA: Materials Research Soc) p 307.

[4] C.J. Pickard, B. Winkler, R.K. Chen, M.C. Payne, M.H. Lee, J.S. Lin, J.A. White, V. Milman, D. Vanderbilt. Phys.Rev. Lett **85**, 5122 (2000).

[5] Chun-Gang Duan, Sabirianov R.F., Mei W.N., Dowben P.A., Jaswal S.S and Tsymbal E.Y. J.Phys. Condens. Matter. **19**, 315220 (2007).

[6] M.De and S.K.De,J.Phys.Chem.Solids **60**, 337 (1999).

[7] Q.J.Sheng, R.R.Cooper, and S.P.Lim, J.Appl.phys. **73**, 5409 (1993).

[8] S.Singh, K.Aneesh and R.K.Singh. J. of Phy. Conf. Series **215**, 012112 (2010).

[9] R.K.Singh. .Phys. Rep. **85**, 259 (1982).

[10] R.K.Singh, S.Singh, Phy. Rev. B **39**, 761 (1989).

[11] M P Tosi,Solid state phys.**16**, 1 (1964).

[12] J. Shanker, V.C. Jain, J.P. Singh, Phy. Rev. B **22**, 1083 (1980).

[13] R.K. Singh, S. Singh. Phy. Rev. B **45**, 1019 (1992).

[14] B. Mayer, H. Anton, E. Bolt, M. Methfessel, J. Sticht, P.C. Schmidt, Intermetallics **11**, 23 (2003).

[15] U.C. Sharma, M.P. Verma., Phys. Stat.sol. (b) **102**, 487 (1980).

[16] W.Cochran CRC Crit. Rev. Sol. State Phys. Mater. Sci, 2, 1 (1971).

[17] G.Pagare, V.Srivastava, S.P.Sanyal, R.K.Singh. Phys.stat.sol.(b) **241**(14), 3193 (2004).

[18] M.R. Vukcevich, phys. Status. Solidi. B **54**, 435 (1972),.

---

*Corresponding author: drsadhna.hpl@gmail.com